Draft version September 17, 2010
Preprint typeset using LaTeX style emulateapj v. 11/10/09

CONSTRAINING THE HARD X-RAY PROPERTIES OF THE QUIET SUN WITH NEW RHESSI OBSERVATIONS

I. G. Hannah
School of Physics & Astronomy,
University of Glasgow, Glasgow G12 8QQ, UK

H. S. Hudson, G. J. Hurford
Space Sciences Laboratory,
University of California, Berkeley, CA, 94720-7450, USA

R. P. Lin
Physics Department & Space Sciences Laboratory,
University of California, Berkeley, CA, 94720-7450, USA;
School of Space Research, Kyung Hee University, Korea

Draft version September 17, 2010

ABSTRACT

We present new RHESSI upper limits in the 3-200 keV energy range for solar hard X-ray emission in the absence of flares and active regions, i.e. the quiet Sun, using data obtained between July 2005 and April 2009. These new limits, substantially deeper than any previous ones, constrain several physical processes that could produce hard X-ray emission. These include cosmic-ray effects and the generation of axions within the solar core. The data also limit the properties of "nanoflares", a leading candidate to explain coronal heating. We find it unlikely for nanoflares involving nonthermal effects to heat the corona because such events would require a steep electron spectrum $E^{-\delta}$ with index $\delta > 5$ extending to very low energies (< 1 keV), into the thermal energy range. We also use the limits to constrain the parameter space of an isothermal model and coronal thin-target emission models (powerlaw and kappa distributions).

Subject headings: elementary particles — Sun: X-rays, gamma rays — Sun: activity — Sun: corona

1. INTRODUCTION

To a hard X-ray telescope much more sensitive than RHESSI (Lin et al. 2002), the quiet Sun, i.e. free of flares and active regions, should appear dark against the diffuse cosmic X-ray sky. But how faint can the solar atmosphere itself be? Intense magnetic fields collect in the network of convective motions at the photosphere, and a wide variety of transient phenomena occur all the time even in the absence of sunspots or other major kinds of solar activity. The high temperature (several MK) of the corona itself has always posed a problem, with abundant literature devoted to finding the source of energy involved in maintaining it. An often cited idea is that of a large number of events too weak to detect individually, but pervading the volume of the corona and extracting the energy of its magnetic field bit by bit – the "nanoflares" discussed by Parker (1988). A nanoflare population may operate in a similar manner to the suggested active-region nanoflares (e.g. Cargill & Klimchuk 1997) or be considerably smaller versions of traditional active-region flares (e.g. Hannah et al. 2008) but they would need to exist in the absence of active regions given that the corona remains consistently hot during quiet periods.

Such short-duration transient heating events, occurring on an Alfvén time scale, would temporarily produce a higher temperature than the mean (greater than a few MK) and the resulting differential emission measure DEM of an ensemble of such events in the steady state must therefore extend to higher temperatures (e.g. Cargill 1994), producing soft X-rays (SXR), emission typically below a few to 10 keV. Or if they operated in a similar manner to active-region flares, where accelerated electrons heat the chromospheric material, then they would produce a faint hard X-ray (HXR) signature via nonthermal bremsstrahlung, emission typically above a few to 10 keV. Either way a quiet-Sun nanoflare population would likely produce SXR and HXR emission above 3 keV, an energy range observable by RHESSI.

Other X-ray observations of the quiet Sun have either provided isothermal model fits to the limiting SXR emission (Peres et al. 2000; Pevtsov & Acton 2001; Sylwester et al. 2010) or upper limits to the HXR emission (Peterson et al. 1966; Feffer et al. 1997). RHESSI uniquely bridges the SXR to HXR energy range and so is an ideal tool to investigate solar thermal and nonthermal emission. However its imaging is optimised for flare observations and so in its normal mode of operation is ill-suited to observing the weak, spatially widespread signal from the quiet Sun. Instead an off-pointing mode of operation was developed termed *fan-beam modulation* (Hannah et al. 2007a), (see further details in §2.1) which allows a weak full-disc signal to be investigated. This produced more stringent upper limits to the quiet Sun X-ray emission between 3-200 keV (Hannah et al.

iain@astro.gla.ac.uk
hudson@ssl.berkeley.edu, hurford@ssl.berkeley.edu
rplin@ssl.berkeley.edu

2007b), covering a wider energy range than previously found (Peterson et al. 1966; Feffer et al. 1997).

In this paper we present a two-fold improvement over this analysis. First we present deeper RHESSI quiet-Sun upper limits found using offpointing data from the whole of the exceptional minimum of Solar Cycle 23, 2005 to 2009 (the previous analysis covered only 2005 to 2006). Secondly we use these limits to investigate the thermal (§3.1) and nonthermal (§3.2) properties of a possible nanoflare population. In the latter case we investigate whether they can satisfy the coronal heating requirement (Withbroe & Noyes 1977). We also consider, in §3.3, the upper limits in the terms of possible coronal thin-target emission.

Outside the domain of solar activity, there are other mechanisms that would produce HXR emission. At some level the high-energy galactic cosmic rays will result in X-ray emissions from the photosphere (e.g. Seckel et al. 1991; MacKinnon 2007). The γ-ray emission from cosmic rays interacting with the solar atmosphere have recently been observed with FERMI (Orlando et al. 2009). The cosmic X-ray background, known to be of extragalactic origin, is bright and has a relatively flat (hard) spectrum. It should be blocked by the solar disk, yet produce a diffuse component via Compton scattering (e.g. Churazov et al. 2008). A well-defined X-ray source could also result from axion production in the core of the Sun, converting via interactions with the magnetic field in the solar atmosphere (Sikivie 1983; Carlson & Tseng 1996). We discuss briefly in §3.4 the interpretation of the RHESSI limits in terms of these other emission mechanisms.

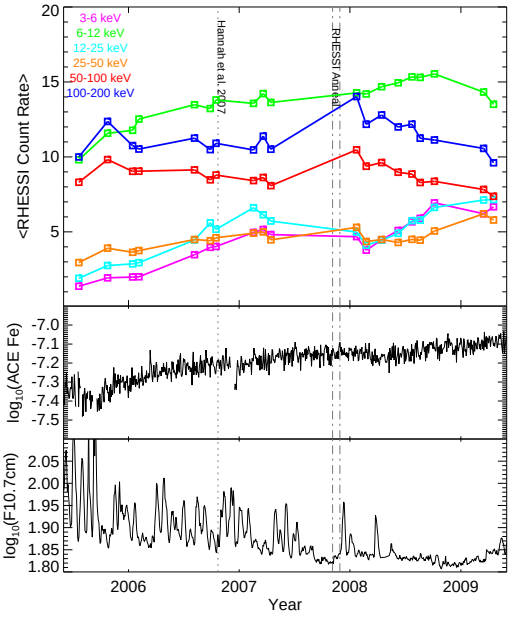

FIG. 1.— Time profile of the *RHESSI* count rate in different energy bands (top panel) averaged over detectors 1,3,4 and 6 and over the five minute intervals used to determine the quiet Sun limits. The vertical line indicates the date up to which the previous analysis had been done (Hannah et al. 2007b). The dot-dash lines indicate *RHESSI*'s first anneal (5-29 November 2007). The middle panel shows the Fe 270-450 MeV/nucleon rate for Galactic Cosmic Rays from ACE/CRIS (Stone et al. 1998). The bottom panel shows the solar 10.7 cm radio flux, adjusted to 1AU (courtesy of the Canadian Space Weather Forecast Centre).

2. RHESSI QUIET SUN DATA

2.1. *Fan-beam Modulation Technique*

RHESSI makes images via a set of nine rotating modulation collimators RMCs, whose resolution range logarithmically between 2.3″ and 183″ (Hurford et al. 2002). Each of the grids also produces a coarser modulation, depending on its thickness, on the order of the angular scale of the whole Sun. To make use of this coarse modulation the spacecraft must point slightly away from the Sun, the optimum effect occurring between 0.4° and 0.9° from disc centre. These operations interrupt the normal RHESSI program of flare observations, so the quiet Sun mode is only used when solar activity is expected to be at its lowest possible level. Data taken during these offpointing periods is then fitted with the expected fan-beam sinusoidal modulation profile of a uniform solar disc sized source (Hannah et al. 2007a), providing a measure of the signal (or emission upper limit) above instrumental and terrestrial background.

In the present analysis we combine the older and newer data. The earlier data consisted of seven intervals between 19 July 2005 and 23 October 2006, as reported by Hannah et al. (2007b). The new data includes all of the RHESSI quiet Sun observations following these, including the solar minimum between Hale Cycles 23 and 24, and comprise an additional twelve periods from 12 February 2007 to 22 April 2009. The total number of observing sessions is 19, spanning 140 days.

For each of the offpointing periods we selected data with the criteria (i) GOES SXR flux levels below the A1 level (10^{-8} Wm^{-2}), (ii) no obvious GOES or RHESSI time variations, and (iii) RHESSI background counting rates at the minima in the latitude dependence due to cosmic radiation (see Figures 1 and 2 in McTiernan (2009)). Each of the selected periods was split into 5 min intervals and then fitted with the expected fan-beam modulation profiles (Hannah et al. 2007a) for each detector and chosen energy band. This selection resulted in 3,428 five-minutes intervals, a total of 11.9 days. We obtained a fitted modulation amplitude for each interval, for each energy band, using the subset of RMCs (numbers 1, 3, 4, and 6) best suited to this technique.

Figure 1 summarises the data in the context of the background cosmic-ray and solar variability. The mean rates are dominated by intrinsic background sources, i.e. not by X-ray fluxes located within the imaging field of view. During the entire interval of the RHESSI quiet Sun observations, the galactic cosmic-ray flux was increasing towards record maximum levels, as shown in the middle panel of the figure, based on Advanced Composition Explorer (ACE) data (Stone et al. 1998). The increase of cosmic rays is as expected from the solar-cycle modulation, and extends beyond the solar activity minimum in late 2008, shown in the bottom panel by the solar 10.7 cm radio flux, also as expected (Mewaldt et al. 2009). The low-energy RHESSI analysis bands, excluding 6-12 keV, appear to show a similar upward trend; this band contains a discrete instrumental spectral feature at about 10 keV. This keV wide feature is present in all detectors during both sunlight and eclipse times and was speculated to be mostly due to the K-line emis-

TABLE 1
THE WEIGHTED MEAN, AND ITS ASSOCIATED STANDARD DEVIATION, OF THE *RHESSI* QUIET SUN PHOTON FLUX. THE PREVIOUS VALUES (HANNAH ET AL. 2007B) ARE GIVEN IN BRACKETS.

Energy keV	Weighted Mean $\times 10^{-4}$ph s^{-1} cm^{-2} keV^{-1}	σ
3–6	-31.17 (330.99)	±170.19 (±207.25)
6–12	5.97 (-5.24)	±4.75 (±8.46)
12–25	0.51 (-0.73)	±0.94 (±1.34)
25–50	0.02 (0.14)	±0.40 (±0.63)
50–100	-0.08 (-0.74)	±0.29 (±0.54)
100–200	-0.01 (-0.79)	±0.22 (±0.42)

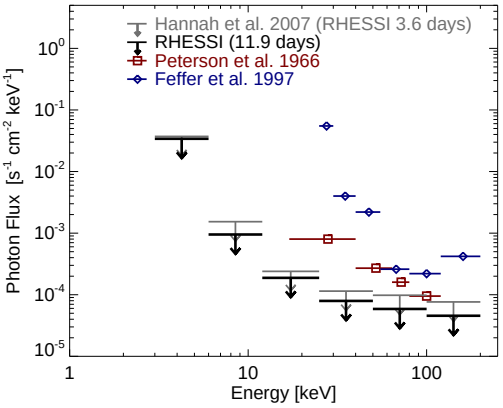

FIG. 2.— The RHESSI upper limits of the quiet Sun photon flux spectrum. The values are the 2σ limits, from the standard deviation of the weighted mean of the four RMCs. The previous results using data during July 2005 to October 2006 is also shown (Hannah et al. 2007b) as are the other HXR upper limits found from Peterson et al. (1966) and Feffer et al. (1997).

sion from radioactive decay in the germanium detectors (Phillips et al. 2006). More specifically, via a private communication with A. Zoglauer and D. Smith, it seems to be a due to cosmic protons causing electron capture decay producing ^{71}Ga fluorescence X-rays at about 10.4 keV.

At the higher energies (above about 50 keV) this cosmic-ray dependence appears to decrease, and we speculate that the RHESSI background at these energies is more closely associated with the trapped radiation around the Earth than with the primary cosmic rays interacting in the Earth's atmosphere and producing secondary radiations detectable at the RHESSI orbital altitude of about 500 km. A further complication is the cumulative effect of radiation damage to RHESSI's unshielded detectors over this period of low solar activity, which increases background noise and reduces detector active volume. Due to this no quiet Sun offpointing occurred in the second half of 2007, before a detector anneal was conducted in November 2007 after which the detector response recovered back to 2005 levels. Similarly, no quiet-Sun offpointing was commanded after April 2009 due to the continued degradation of RHESSI's detectors, despite the prolonged solar minimum. A second detector anneal in March 2010 greatly improved the performance of the detectors, returning it to early mission levels, but the Sun was no longer quiet.

For each energy band and detector the weighted mean and standard deviation of the fitted amplitudes with their associated errors is calculated for all the time intervals. These values are then converted from counts flux to photon flux using the diagonal elements of RHESSI's detector response matrix. A final amplitude and statistical error is then calculated, again using the weighted mean, from the four values with errors per energy band. We find no significant signal in any energy channel. Table 1 gives the results in comparison with the initial data of Hannah et al. (2007b). As expected, the further observations has substantially reduced the derived limits, and the >1 σ detection found previously in the lowest (3-6 keV) band has become simply a limit. Figure 2 shows these results graphically, in comparison with the earlier results (Peterson et al. 1966; Feffer et al. 1997). These limits now become the deepest limits for solar hard X-ray emission yet reported.

3. INTERPRETATIONS

3.1. *Isothermal Emission*

The most natural interpretation of these observations would be as limits on thermal sources in the corona, mainly free-free and free-bound continuum in the HXR range. RHESSI also detects bound-bound emissions of Fe and Ni in the 6-8 keV range (e.g. Phillips 2004). Although the bulk of the corona is too cool to produce thermal emission in the RHESSI range above 3 keV, localised higher temperature emission (i.e. from bright points) could easily provide emission in this energy range.

In the left panel of Figure 3 we show the new RHESSI upper limits in the context of previous quiet Sun and non-flaring active region observations. Yohkoh/SXT produced a limiting value for the SXR quiet Sun (Pevtsov & Acton 2001) and this was used to find suitable isothermal model fits (Peres et al. 2000). The SphinX observations of the end of Solar Cycle 23 have given preliminary estimates of a low, steady level of X-ray emission that may provide the best characterisation of the background coronal emission (Sylwester et al. 2010). An isothermal fit was also made to this emission, again shown in Figure 3. In both cases these quiet Sun isothermal models are consistently lower than the RHESSI upper limits. Also shown are the isothermal models fits during non-flaring quiescent active region times from SphinX (Sylwester et al. 2010) and RHESSI (McTiernan 2009). As expected, the RHESSI upper limits are lower than the quiescent active region emission.

In the right panel of Figure 3 we have calculated the maximum emission measure as a function of isothermal temperature which is consistent with the RHESSI quiet Sun limits and the SXT constraint (Pevtsov & Acton 2001). We find that this can be fitted with a polynomial of form

$$\log EM = 52.97 - 15.25 \log T + 5.24 \log^2 T \qquad (1)$$

where T is in units of MK and EM is in units of cm^{-3}. Above about 5 MK the emission measure is strongly constrained by the RHESSI upper limits, with a maximum $< 10^{44}$ cm^{-3}. For reference the standard Withbroe (1988) semi-empirical models of the solar wind, includ-

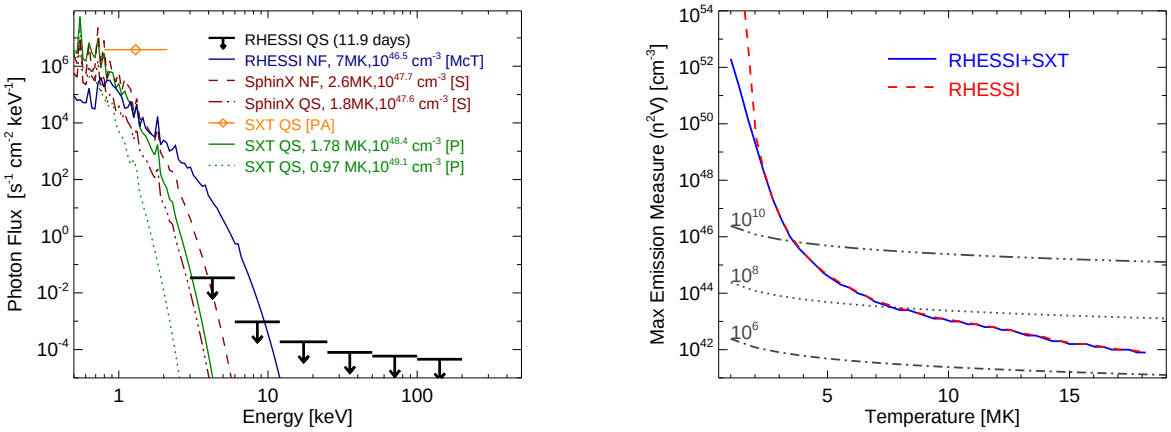

FIG. 3.— (*Left*) The *RHESSI* upper limits compared to previously found thermal emission from the quiet Sun ([PA] Pevtsov & Acton (2001), [P] Peres et al. (2000), [S] Sylwester et al. (2010)) and non-flaring active regions ([S] Sylwester et al. (2010), [McT] McTiernan (2009)). (*Right*) The maximum emission measure as a function of temperature such that an isothermal model produces a X-ray spectrum less than the *RHESSI* and *Yohkoh/SXT* limits (Pevtsov & Acton 2001), shown in left panel. The area under the curve is the possible parameter space consistent with the observations. The dotted and dash-dotted grey lines indicate the emission measure and temperature combination consistent with the coronal heating requirement (Withbroe & Noyes 1977) with different background plasma densities ($n = 10^{10}, 10^{8}, 10^{6}$ cm^{-3} from top to bottom).

ing the corona, have emission measures in the range 0.8-9×10^{49} cm^{-3}, with peak temperatures in the range 1.42-1.64 MK and so are consistent with our limits. These however are solar-wind models and therefore almost certainly underestimate both the temperature and the emission measure of the steady-state quiet corona.

An additional constraint to the isothermal parameter space can be obtained by considering the energy content being consistent with the coronal heating requirement (Withbroe & Noyes 1977). As a function of temperature and for three assumed coronal densities ($n = 10^{10}, 10^{8}, 10^{6}$ cm^{-3}) we have estimated the emission measures, over plotting this in Figure 3. The lowest density provides little further constraint but the high densities suggest a maximum temperature of 7MK and about 4MK is possible for densities of $n = 10^{8}$ cm^{-3} and $n = 10^{10}$ cm^{-3} respectively.

3.2. *Nonthermal Thick-Target Emission*

The development of a solar flare involves nonthermal energy release, marked for example by HXR and microwave emission, and the consequent increase of coronal pressure in the flaring region. The pressure increase results from the evaporation of chromospheric material to form the hot coronal plasma responsible for SXR emission. The relationship between the nonthermal component and the thermal component is well-understood observationally; the peak SXR and HXR fluxes scale approximately linearly together within a factor of 10 or so over several decades (e.g. Veronig et al. 2001). It is therefore worthwhile to analyse our limits in terms of nonthermal bremsstrahlung, especially since we do not know whether the flare relationship of nonthermal and thermal processes holds for the quiet corona.

We assume that there is a single power-law distribution of electrons $f(E) \propto E^{-\delta}$ in the quiet Sun that produces HXR emission via thick-target bremsstrahlung (Brown 1971). Such a model is a good basis for our limits since the corona contains mainly closed magnetic fields, and our long integration times exceed the collisional loss times of electrons trapped within them. This model has four parameters: the spectral index δ, the energy range over which the power-law extends (low energy cut off $E_{\rm C}$ to maximum energy $E_{\rm M}$) and the total integrated electron flux, $N = \int f(E)dE$ [electrons s^{-1}]. We fix the maximum energy at $E_{\rm M} = 1$ MeV as for the steep spectra and photon energy range we are considering it has little effect. The remaining three parameters can be further consolidated if we require a match to the assumed coronal heating requirement $P_{\rm WN} = 9 \times 10^{27}$ erg s^{-1} (Withbroe & Noyes 1977). The total integrated electron flux N can then be removed by rewriting it in terms of the power ($P = \int f(E)EdE$), i.e.

$$N = 1.6 \times 10^{-9} \frac{P_{\rm WN}(\delta - 2)}{E_{\rm C}(\delta - 1)} \quad \text{electrons s}^{-1}, \qquad (2)$$

where $E_{\rm C}$ is in keV. We can then investigate the possible range of spectral index δ and low energy cutoff $E_{\rm C}$ that produce a thick-target bremsstrahlung spectrum $I(\epsilon)$ lower than the RHESSI limits. Some example HXR spectra are shown in the left panel of Figure 4 which are consistent with the coronal heating requirement and the RHESSI upper limits, using the numerical implementation of Holman (2003). We can find the maximum possible low energy cutoff that is possible for a range of spectral indices and this is shown in the right panel of Figure 4. An additional parameter-space constraint is of $E_{\rm C} = 5kT/2$ as determined by the coronal thermal plasma temperature T (Emslie 2003). With this we find that only steep electron spectra ($\delta > 5$) are possible and that they extend down to very low electron energies close to the thermal regime. Note that we have assumed that the upper limits are solely due to nonthermal emission. An additional, and highly likely, thermal component would reduce the nonthermal parameter-space even further. We thus find a nanoflare coronal heating model based on flares similar to nonthermal active region flares to be implausible.

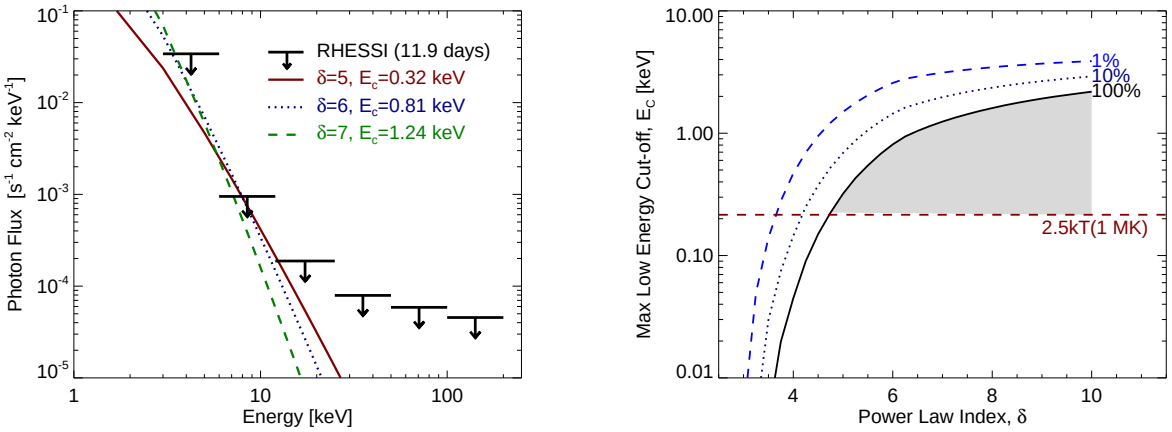

FIG. 4.— (*Left*) The *RHESSI* upper limits compared to thick-target model X-ray spectra from a power-law of accelerated electrons of spectral index δ above cutoff energy E_c and consistent with the coronal heating requirement (Withbroe & Noyes 1977). (*Right*) The possible nonthermal parameters that could provide either 100%, 10% or 1% of the coronal heating requirement (Withbroe & Noyes 1977) while producing an X-ray spectrum below the *RHESSI* limits (area below each curve). The horizontal line indicates the possible lower limit to E_C based on a typical coronal temperature (Emslie 2003).

3.3. *Thin-Target Emission*

Another likely emission mechanism to produce quiet Sun HXRs is via a coronal thin-target process (e.g. Lin & Hudson 1976), where energised electrons would continuously emit via bremsstrahlung interactions with the coronal plasma but would lose little energy doing so (unlike the complete energy loss through collisions with the denser chromosphere in the thick-target case §3.2). For these models we cannot use the coronal heating requirement to constrain the parameter space as there is no substantial energy loss to heat the background plasma. We consider two models both of which are functions of three parameters. We again consider a power law distribution of electrons with spectral index δ above a low energy cut-off E_C (extending up to energy of 1 MeV), this time normalised by the product of the plasma density, volume of emitting plasma and integrated electrons flux (nVN [cm^{-2} s^{-1}]). The parameter space (E_C, δ) of this model, for different values of the normalisation, that produces thin-target emission $I(\epsilon)$ less than the RHESSI upper limits are shown in Figure 5. As the normalisation factor increases the maximum low energy cut-off sharply decreases, requiring $\delta > 7$ for $nVN = 10^{59}$ cm^{-2}s^{-1} again once the additional constraint of Emslie (2003) is included.

The second model we consider is a kappa distribution which can fit observed in-situ solar wind distribution and some coronal flare spectra (Kašparová & Karlický 2009). The distribution is a function of emission measure nVN_κ (not the same as the isothermal emission measure n^2V as N_κ, the electron density in the kappa distribution, is included with the background plasma density n) temperature T and the kappa parameter κ, numerically implemented using the version from Kašparová & Karlický (2009). The kappa parameter adds a high-energy tail to the thermal Maxwellian, approaching a powerlaw at high energies for low κ. The emission measure temperature parameter space for various values of κ that produce thin-target emission $I(\epsilon)$ consistent with the RHESSI limits are shown in the right panel of Figure 5. Low values of $\kappa < 6$ (a flat tail) greatly reduce the possible emission measure since we have more high energy electrons in the tail to produce X-rays. For larger values $\kappa \geq 20$ we approach the isothermal constraints shown in Figure 3.

3.4. *Axions*

The flux of axions thought to be produced in the Sun's core have a mean energy of 4.2 keV in a roughly blackbody distribution (van Bibber et al. 1989; Andriamonje et al. 2007) and convert directly to photons of the same energy with probability proportional to $(\int B_\perp dl)^2$ (the perpendicular magnetic field encountered) and $g^2_{a\gamma\gamma}$, an unknown coupling constant. The unique parameter space available to the RHESSI limits further constrain this coupling. The limits in 3-6 keV presented in this paper are about 20% smaller than those from the previous analysis (Hannah et al. 2007b). Assuming that these limits are exclusively due to axions then we find our limits to be lower than the X-ray emission predicted for light axion conversion in a simple dipole field with $g_{a\gamma\gamma} = 10^{-10}$ GeV^{-1} (Carlson & Tseng 1996). A smaller $g_{a\gamma\gamma}$ or a modified magnetic field model could produce X-ray emission within our limits. For the scenario of massive Kaluza-Klein axions our new X-ray upper limits still produce $g_{a\gamma\gamma} \ll 6 \times 10^{-15}$ GeV^{-1}, using the method of Zioutas et al. (2004), since the X-ray luminosity is proportional to $g^4_{a\gamma\gamma}$.

A better treatment of this problem would require more complete knowledge of the perpendicular magnetic fields encountered by the axions fleeing the Sun. This field would not be expected to vary during solar minimum except for statistical fluctuations of the magnetic field in the quiet Sun. In the presence of higher levels of activity, and stronger localised magnetic fields, strong spatial and temporal variations would become evident. To the extent that the axion spectral signature cannot be disentangled, the normal mechanisms of solar magnetic activity could easily outweigh the axion source intensity.

4. CONCLUSIONS

The RHESSI observations reported here give the best upper limits yet on solar X-ray emission, at the quietest times, above 3 keV. These limits constrain models of

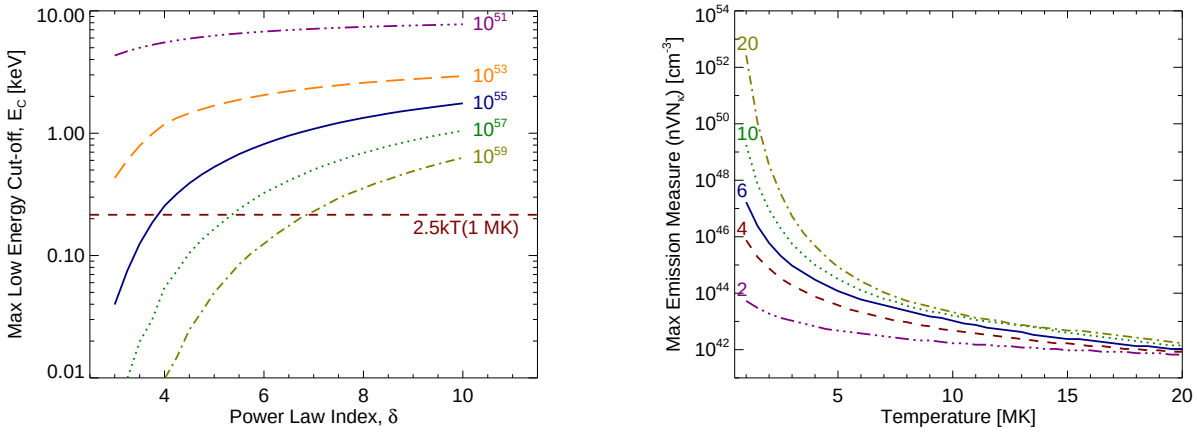

FIG. 5.— The possible parameter space for (*left*) a power-law distribution of accelerated electrons and (*right*) a kappa distribution that produce thin-target X-ray emission consistent with the RHESSI upper limits. The different lines denote the maximum possible in the parameter space for different values of the (*left*) normalisation parameter nVN and (*right*) kappa parameter κ. (*Left*) The horizontal line indicates the possible lower limit to E_C based on a typical coronal temperature (Emslie 2003).

coronal heating that require high temperatures or non-thermal particles and possible coronal thin-target emission. In all instances this was considered in terms of a spatially and temporally averaged emission, a "typical" nanoflare, whereas a distribution of nanoflares could easily produce individual events brighter than the RHESSI upper limits for short periods of time. For the high-temperature tail of a DEM consistent with nanoflare heating, we find that the fraction of emission measure above 5 MK must be $\lesssim 10^{-6}$ of the peak of the DEM needed for the quiet corona, crudely estimated at 2×10^{50} cm^{-3} for a coronal base density of 10^9 cm^{-3}. Nanoflare models (e.g. Klimchuk et al. 2008) involve many interrelated free parameters at present, and we hope that our strong limits will be incorporated into future theoretical work. Further parameter-space constraints result if we interpret our limits in terms of non-thermal bremsstrahlung from accelerated electrons. Here the limits force the spectral index δ to be steeper than about 5 for any physically meaningful low-energy cutoff energy E_c. With this nonthermal interpretation, heating via particle acceleration, we demonstrated that it was unlikely that nanoflares could heat the corona in a manner akin to heating in ordinary flares.

The RHESSI solar observations we report here, though the best ever achieved in the HXR range, could be greatly improved since RHESSI (and most other solar instruments) are not optimised for faint sources. One approach would be using focusing optics, allowing quiet regions of the corona to be isolated with high sensitivity and wide dynamic range, possible with technology such as *FOXSI* (Krucker et al. 2009) sounding rocket and NuSTAR (Harrison et al. 2010) satellite instruments, both scheduled for launch. Such observations would not only allow us to investigate the existence and nature of a quiet Sun accelerated electron population but would greatly benefit our understanding of energy release and transport processes in active-region flares.

5. ACKNOWLEDGEMENTS

IGH is supported by a STFC rolling grant and by the European Commission through the SOLAIRE Network (MTRN-CT-2006-035484). This work was supported in part by NASA contract NAS5-98033. R. Lin was also supported in part by the WCU grant (No. R31-10016) funded by the Korean Ministry of Education, Science and Technology.

REFERENCES

Andriamonje, S., 60 co-authors, & the (CAST Collaboration). 2007, Journal of Cosmology and Astro-Particle Physics, 4, 10
Brown, J. C. 1971, Sol. Phys., 18, 489
Cargill, P. J. 1994, ApJ, 422, 381
Cargill, P. J., & Klimchuk, J. A. 1997, ApJ, 478, 799
Carlson, E. D., & Tseng, L. S. 1996, Physics Letters B, 365, 193
Churazov, E., Sazonov, S., Sunyaev, R., & Revnivtsev, M. 2008, MNRAS, 385, 719
Emslie, A. G. 2003, ApJ, 595, L119
Feffer, P. T., Lin, R. P., Slassi-Sennou, S., McBride, S., Primbsch, J. H., Zimmer, G., Pelling, R. M., Pehl, R., Madden, N., Malone, D., Cork, C., Luke, P., Vedrenne, G., & Cotin, F. 1997, Sol. Phys., 171, 419
Hannah, I. G., Christe, S., Krucker, S., Hurford, G. J., Hudson, H. S., & Lin, R. P. 2008, ApJ, 677, 704
Hannah, I. G., Hurford, G. J., Hudson, H. S., & Lin, R. P. 2007a, Review of Scientific Instruments, 78, 10
Hannah, I. G., Hurford, G. J., Hudson, H. S., Lin, R. P., & van Bibber, K. 2007b, ApJ, 659, L77
Harrison, F., Boggs, S., Christensen, F., Craig, W., Hailey, C., Stern, D., Zhang, W., & NuSTAR Science Team. 2010, in Bulletin of the American Astronomical Society, Vol. 41, Bulletin of the American Astronomical Society, 737–+
Holman, G. D. 2003, ApJ, 586, 606
Hurford, G. J., Schmahl, E. J., Schwartz, R. A., Conway, A. J., Aschwanden, M. J., Csillaghy, A., Dennis, B. R., Johns-Krull, C., Krucker, S., Lin, R. P., McTiernan, J., Metcalf, T. R., Sato, J., & Smith, D. M. 2002, Sol. Phys., 210, 61
Kašparová, J., & Karlický, M. 2009, A&A, 497, L13
Klimchuk, J. A., Patsourakos, S., & Cargill, P. J. 2008, ApJ, 682, 1351
Krucker, S., Christe, S., Glesener, L., McBride, S., Turin, P., Glaser, D., Saint-Hilaire, P., Delory, G., Lin, R. P., Gubarev, M., Ramsey, B., Terada, Y., Ishikawa, S., Kokubun, M., Saito, S., Takahashi, T., Watanabe, S., Nakazawa, K., Tajima, H., Masuda, S., Minoshima, T., & Shomojo, M. 2009, in Society of Photo-Optical Instrumentation Engineers (SPIE) Conference Series, Vol. 7437, Society of Photo-Optical Instrumentation Engineers (SPIE) Conference Series

Lin, R. P., Dennis, B. R., Hurford, G. J., Smith, D. M., Zehnder, A., Harvey, P. R., Curtis, D. W., Pankow, D., Turin, P., Bester, M., Csillaghy, A., Lewis, M., Madden, N., van Beek, H. F., Appleby, M., Raudorf, T., McTiernan, J., Ramaty, R., Schmahl, E., Schwartz, R., Krucker, S., Abiad, R., Quinn, T., Berg, P., Hashii, M., Sterling, R., Jackson, R., Pratt, R., Campbell, R. D., Malone, D., Landis, D., Barrington-Leigh, C. P., Slassi-Sennou, S., Cork, C., Clark, D., Amato, D., Orwig, L., Boyle, R., Banks, I. S., Shirey, K., Tolbert, A. K., Zarro, D., Snow, F., Thomsen, K., Henneck, R., McHedlishvili, A., Ming, P., Fivian, M., Jordan, J., Wanner, R., Crubb, J., Preble, J., Matranga, M., Benz, A., Hudson, H., Canfield, R. C., Holman, G. D., Crannell, C., Kosugi, T., Emslie, A. G., Vilmer, N., Brown, J. C., Johns-Krull, C., Aschwanden, M., Metcalf, T., & Conway, A. 2002, Sol. Phys., 210, 3

Lin, R. P., & Hudson, H. S. 1976, Sol. Phys., 50, 153

MacKinnon, A. L. 2007, A&A, 462, 763

McTiernan, J. M. 2009, ApJ, 697, 94

Mewaldt, R. A., Davis, A. J., Lave, K. A., Leske, R. A., Wiedenbeck, M. E., Binns, W. R., Christian, E. R., Cummings, A. C., de Nolfo, G. A., Israel, M. H., Stone, E. C., & von Rosenvinge, T. T. 2009, AGU Fall Meeting Abstracts, C8+

Orlando, E., Giglietto, N., & for the Fermi Large Area Telescope Collaboration. 2009, ArXiv e-prints

Parker, E. N. 1988, ApJ, 330, 474

Peres, G., Orlando, S., Reale, F., Rosner, R., & Hudson, H. 2000, ApJ, 528, 537

Peterson, L. E., Schwartz, D. A., Pelling, R. M., & McKenzie, D. 1966, J. Geophys. Res., 71, 5778

Pevtsov, A. A., & Acton, L. W. 2001, ApJ, 554, 416

Phillips, K. J. H. 2004, ApJ, 605, 921

Phillips, K. J. H., Chifor, C., & Dennis, B. R. 2006, ApJ, 647, 1480

Seckel, D., Stanev, T., & Gaisser, T. K. 1991, ApJ, 382, 652

Sikivie, P. 1983, Physical Review Letters, 51, 1415

Stone, E. C., Cohen, C. M. S., Cook, W. R., Cummings, A. C., Gauld, B., Kecman, B., Leske, R. A., Mewaldt, R. A., Thayer, M. R., Dougherty, B. L., Grumm, R. L., Milliken, B. D., Radocinski, R. G., Wiedenbeck, M. E., Christian, E. R., Shuman, S., Trexel, H., von Rosenvinge, T. T., Binns, W. R., Crary, D. J., Dowkontt, P., Epstein, J., Hink, P. L., Klarmann, J., Lijowski, M., & Olevitch, M. A. 1998, Space Science Reviews, 86, 285

Sylwester, J., Kowalinski, M., Gburek, S., Siarkowski, M., Kuzin, S., Farnik, F., Reale, F., & Phillips, K. J. H. 2010, EOS Transactions, 91, 73

van Bibber, K., McIntyre, P. M., Morris, D. E., & Raffelt, G. G. 1989, Phys. Rev. D, 39, 2089

Veronig, A., Vršnak, B., Temmer, M., Magdalenić, J., & Hanslmeier, A. 2001, Hvar Observatory Bulletin, 25, 39

Withbroe, G. L. 1988, ApJ, 325, 442

Withbroe, G. L., & Noyes, R. W. 1977, ARA&A, 15, 363

Zioutas, K., Dennerl, K., DiLella, L., Hoffmann, D. H. H., Jacoby, J., & Papaevangelou, T. 2004, ApJ, 607, 575